

A Decentralized Pilot Assignment Methodology for Scalable O-RAN Cell-Free Massive MIMO

Myeung Suk Oh, *Student Member, IEEE*, Anindya Bijoy Das, *Member, IEEE*, Seyyedali Hosseinalipour, *Member, IEEE*, Taejoon Kim, *Senior Member, IEEE*, David J. Love, *Fellow, IEEE*, and Christopher G. Brinton, *Senior Member, IEEE*

Abstract

Radio access networks (RANs) in monolithic architectures have limited adaptability to supporting different network scenarios. Recently, open-RAN (O-RAN) techniques have begun adding enormous flexibility to RAN implementations. O-RAN is a natural architectural fit for cell-free massive multiple-input multiple-output (CFmMIMO) systems, where many geographically-distributed access points (APs) are employed to achieve ubiquitous coverage and enhanced user performance. In this paper, we address the decentralized pilot assignment (PA) problem for scalable O-RAN-based CFmMIMO systems. We propose a low-complexity PA scheme using a multi-agent deep reinforcement learning (MA-DRL) framework in which multiple learning agents perform distributed learning over the O-RAN communication architecture to suppress pilot contamination. Our approach does not require prior channel knowledge but instead relies on real-time interactions made with the environment during the learning procedure. In addition, we design a codebook search (CS) scheme that exploits the decentralization of our O-RAN CFmMIMO architecture, where different codebook sets can be utilized to further improve PA performance without any significant additional complexities. Numerical evaluations verify that our proposed scheme provides substantial computational scalability advantages and improvements in channel estimation performance compared to the state-of-the-art.

Index Terms

M. S. Oh, A. B. Das, D. J. Love, and C. G. Brinton are with the School of Electrical and Computer Engineering, Purdue University, West Lafayette, IN, 47907 USA (e-mail: {oh223, das207, djlove, cgb}@purdue.edu).

S. Hosseinalipour is with the Department of Electrical Engineering, University at Buffalo, NY, 14260 USA (email: alipour@buffalo.edu).

T. Kim is with the Department of Electrical Engineering and Computer Science, the University of Kansas, Lawrence, KS, 66045 USA (email: taejoonkim@ku.edu).

Open-RAN (O-RAN), cell-free massive MIMO, deep reinforcement learning, pilot assignment.

I. INTRODUCTION

A. Open Radio Access Network (O-RAN)

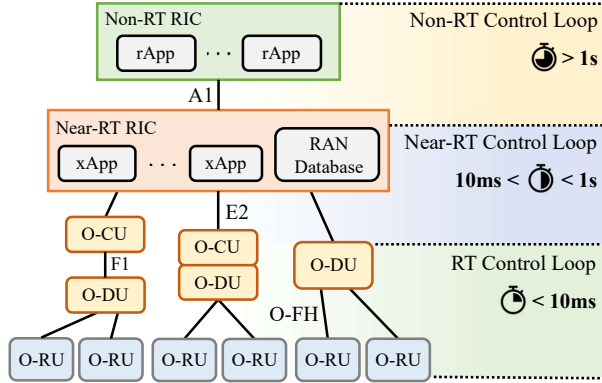
Next generation wireless technologies will likely employ many dispersed radio access networks (RANs) for ubiquitous coverage and enhanced user performance [1], [2]. However, interconnecting different RANs to create one seamless network requires well-defined network functions and interfaces which are flexible in their integration capability. Recently, the evolution of software-defined open RAN (O-RAN) solutions have added enormous flexibility to the implementation of current 5G networks [3]–[5] and development of emerging 6G networks. O-RAN offers software-defined disaggregation on virtual network functions (VNFs) and necessary interfaces to support their coordination, allowing system implementations that are adaptive to various architectural settings. With this openness and flexibility, O-RAN promotes interoperability across different RAN vendors and allows network operators to adapt to different wireless environments.

O-RAN adopts the functional split defined in 3GPP [6] and defines three distinct units [7]: the open central unit (O-CU), open distributed unit (O-DU), and open radio unit (O-RU). Moreover, O-RAN operation is divided into three different control loops [7]: the real-time (RT), near-RT, and non-RT loops executing at different time-scales. The resulting O-RAN architecture, and standard names of interfaces between these elements which enable practical implementations of many RAN operations, are depicted in Fig. 1a.

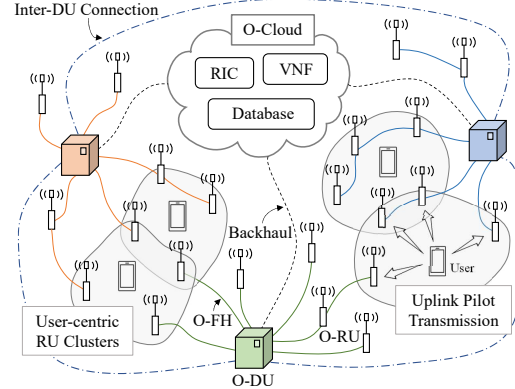
O-RAN offers two types of RAN intelligent controllers (RICs) [7] as shown in Fig. 1a: near-RT RIC and non-RT RIC. Each of these RICs handles tasks manageable in different time-scales. O-RAN offers virtualization of both RICs, which promotes flexibility in implementing data-driven intelligence tasks that will be key components of emerging wireless networks. Various operations can be implemented via custom third-party applications called *xApps/rApps* [7], allowing RICs to be much more accessible to the public. In this work, we will consider the implementation of machine learning (ML) algorithms over these RICs to optimize pilot signal assignments.

Due to these aforementioned advantages offered by O-RAN, a number of opportunities to utilize O-RAN on future wireless technologies seem promising, some of which are:

- *Massive multiple-input multiple-output (MIMO) beamforming (BF)*: To implement ML-based BF strategies that handle both latency-intensive (e.g., RT beam selection) and data-intensive



(a) O-RAN architecture with different types of control loops.



(b) A decentralized CFmMIMO system realized in O-RAN.

Fig. 1: Illustrations of O-RAN architecture (left) and decentralized O-RAN CFmMIMO system (right).

(e.g., policy update via real-world dataset) tasks is challenging, and O-RAN provides a platform for realizing their framework [8]–[10]. ML tasks are implemented in RICs, and BF operation can be split over O-RU and O-DU (e.g., option 7.2x [11]) to maximize computational efficiency.

- *Unmanned aerial vehicle (UAV) network*: UAVs are typically deployed in dynamic environments (e.g., emergency rescue and aerial surveillance [12]), where the network infrastructure is required to be extremely flexible and adaptive. Flexibility and interoperability offered by O-RAN can be exploited to meet this architectural need [13], [14].
- *Localization via channel charting*: Channel charting is a data-driven localization technique [15] that maps a user to radio geometry using channel information. For the practical implementation of channel charting, O-RAN can offer a balanced distribution of heavy computational load coming from the data that is consistently collected and updated for each user.

B. Cell-free Massive MIMO

One innovative idea to address the shortcomings of 5G cellular networks is to remove cell boundaries using many dispersed transmission/reception points. This idea falls within the academic definition of cell-free massive MIMO (CFmMIMO) [16]–[18]. By deploying many geo-distributed access points (APs), CFmMIMO system alleviates the existing cell-edge problems by substantially improving both the reliability [19] and energy efficiency [20] compared to cellular massive MIMO. These enhancements are due to the user-centric paradigm offered by CFmMIMO, where a group of APs are dynamically selected to form a cluster to serve each user.

In early CFmMIMO literature, a system with APs connected to a single processing unit (PU) was considered for centralized operation. However, in a scalable system where the number of users

and APs grow large, the resulting complexity becomes prohibitive [21]. Thus, CFmMIMO with multiple decentralized PUs (Fig. 1b), each of which is connected to a disjoint subset of APs, has been introduced to consider scalability [21]–[24]. The decentralization allows the system to scale but still be practical by reducing computational and fronthaul load on each PU [18]. Nevertheless, implementing centralized CFmMIMO techniques (e.g., signal adaptation and resource allocation) into a decentralized architecture is a challenging task.

C. CFmMIMO Pilot Assignment Problem

In CFmMIMO, reliable channel estimation at both transmitter and receiver is absolutely critical to facilitate advanced diversity and signal processing techniques. For channel estimation, a set of orthogonal pilots are used. However, when the number of users grows beyond the number of available pilots, some users must share their pilots with others, leading to pilot contamination (PC) that can significantly degrade the channel estimation performance [25]. To cope with PC, various pilot assignment (PA) methods have been studied in the CFmMIMO literature [26]–[32].

In [26], a greedy PA scheme with iterative pilot updates was proposed to mitigate PC. A dynamic pilot reuse scheme to acquire a set of user-pairs for pilot sharing was proposed in [28]. In [29], a user-group PA strategy, in which the same pilot is assigned to users with minimum overlapping APs, was proposed. Other methods to solve the PA problem include k-means clustering [27], graph coloring [31], tabu-search [30], and Hungarian [32] algorithms.

These prior works [26]–[32], however, require a centralized processing for PA and thus are not scalable computationally. They also utilize closed-form expressions derived from Bayesian estimation, requiring any relevant information (e.g., pathloss) to be known a priori. For large-scale systems, especially under a dynamic environment, accurate prior information is often not available, underscoring the need to develop a PA scheme that does not require prior knowledge.

D. Overview of Methodology and Contributions

Motivated by the aforementioned challenges, we focus on PA in scalable CFmMIMO systems. As CFmMIMO deploys a large number of APs for ubiquitous coverage, it is crucial to maintain a great level of implementation flexibility and interoperability across different RANs for scalability. Hence, we propose to design our CFmMIMO system in O-RAN architecture. As O-RAN keeps balance in operational complexities and computational loads via functional split along the network (i.e., O-RU/DUs and RICs), O-RAN becomes a natural solution for scalable CFmMIMO systems.

Based on the O-RAN CFmMIMO system, we formulate a decentralized PA problem and develop a learning-based PA scheme to solve it. In doing so, we resort to multi-agent deep reinforcement learning (MA-DRL) framework, in which a group of agents individually perform their learning that provides a low-complexity solution without an explicit training stage [33]–[35]. Our PA scheme is designed to operate in the near-RT RIC of O-RAN.

We summarize the key contributions of our work as below.

- We design our CFmMIMO system based on the O-RAN architecture (Sec. II). We specifically focus on channel estimation and pilot allocation models considering practical aspects (e.g., fronthaul overhead and operational complexity by each functional unit), which can be adopted to the O-RAN CFmMIMO systems.
- We design a Markov game model (Sec. III-C) for our MA-DRL which leads to an efficient solution for our decentralized PA problem. In particular, we formulate our reward based on observations that are directly measurable at the O-RUs. Thus, our scheme does not require prior knowledge of channel statistics, which is different from previous PA algorithms [26]–[32].
- Leverage the availability of RICs, we propose a novel learning-based PA scheme (Sec. III-D) aiming to minimize the total mean squared error (MSE) across the users. By adopting the distributed learning framework of MA-DRL, our scheme provides low-complexity PA solutions and therefore offers scalability to support large-scale systems.
- Utilizing the decentralization of our system, we consider two effective ways to improve the PA performance: (i) inter-DU message passing for observation sharing and (ii) low-complexity codebook search (CS) algorithm (Sec. III-E) that jointly operates with our PA scheme. Numerical results verify that these approaches can further improve the PA performance.
- We show that our PA scheme can maintain its performance over a mobile environment, which is possible due to (i) the DRL framework that naturally performs adaptive learning and (ii) the CS algorithm with iterative greedy search. Previous PA methods only consider a static environment and do not address the user mobility.
- We numerically evaluate (Sec. IV) the performance of our PA scheme against the state-of-the-art [30], [32] in both channel estimation performance and computational complexity. The results show that our scheme outperforms the benchmarks in terms of sum-MSE and scalability.

II. SYSTEM MODEL AND PROBLEM FORMULATION

In this section, we first describe the CFmMIMO system realized in O-RAN architecture (Sec. II-A). Then, after describing the channel model (Sec. II-B), we provide details on codebook-based channel estimation (Sec. II-C) and formulate our decentralized PA problem (Sec. II-D).

A. CFmMIMO Configuration in O-RAN Architecture

We consider M single-antenna O-RUs and U O-DUs collected in sets $\mathcal{M} = \{1, 2, \dots, M\}$ and $\mathcal{U} = \{1, 2, \dots, U\}$, respectively. We assume each O-RU is connected to one of the O-DUs in \mathcal{U} via an open fronthaul (O-FH) connection. We define $\mathcal{M}_u^{\text{DU}} \subseteq \mathcal{M}$ as the set of O-RUs connected to O-DU $u \in \mathcal{U}$. We assume inter-DU connections [36] to form RU clusters that are fully user-centric since the users can be served by RUs from different sets of $\mathcal{M}_u^{\text{DU}}$. We focus our work on the PA task while making an assumption that O-FH and inter-DU connections are error-free with no delay. Our O-RAN CFmMIMO system is illustrated in Fig. 1b.

Here, we have our O-DUs connected to O-Cloud [7] via backhaul network (Fig. 1b). O-Cloud is the cloud computing platform that supports the virtualized network functions (VNFs) within O-RAN, which include RICs. In designing our PA scheme, we specifically focus on the near-RT RIC that communicates with O-DUs via E2 interface (Fig. 1a). Now, within the near-RT RIC, we assume U independent learning agents, each of which has a one-to-one correspondence to one of the O-DUs in the system. Note that we assume multiple agents to fully impose decentralization on our system. Each agent in near-RT RIC conducts local learning through the O-DU and O-RUs connected. In addition, we consider a single non-RT RIC interacting with the near-RT RIC via A1 interface (Fig. 1a), which is responsible for learning model updates of near-RT RIC.

Next, we consider K single-antenna users in a set $\mathcal{K} = \{1, 2, \dots, K\}$. For each user k , a user-centric RU cluster is formed such that only $M_k^{\text{UE}} \ll M$ O-RUs are engaged to serve the user, where we define $\mathcal{M}_k^{\text{UE}} \subset \mathcal{M}$ to be the set of O-RUs serving user $k \in \mathcal{K}$ (i.e., $M_k^{\text{UE}} = |\mathcal{M}_k^{\text{UE}}|$ where $|\cdot|$ denotes the set cardinality). Each $\mathcal{M}_k^{\text{UE}}$ is assumed to be selected and updated using a procedure independent from our PA. (e.g., radio resource control (RRC) setup procedure [37]). We also define $\mathcal{K}_m^{\text{RU}} \subset \mathcal{K}$ to be the set of users served by O-RU $m \in \mathcal{M}$.

Since we have U multiple agents performing PA, each user $k \in \mathcal{K}$ must belong to one of these agents. To develop user-to-agent pairings, we consider two different types of users: (i) user k whose $\mathcal{M}_k^{\text{UE}}$ is connected to a single O-DU u , i.e., $\mathcal{M}_k^{\text{UE}} \subseteq \mathcal{M}_u^{\text{DU}}$, which we simply pair that user

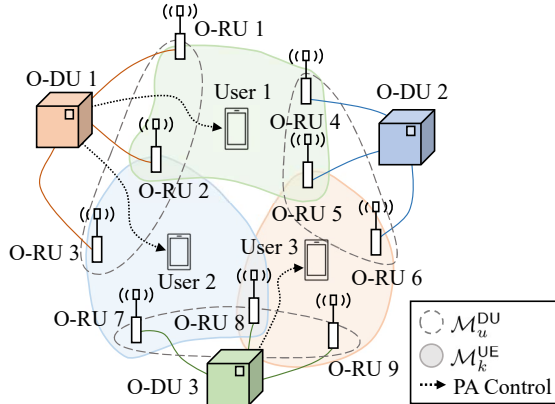


Fig. 2: A list of our defined sets and their visual examples for the given decentralized cell-free O-RAN layout.

k to the corresponding agent u , and (ii) user k whose $\mathcal{M}_k^{\text{UE}}$ consists of O-RUs from different O-DUs. For the second type, a serving O-DU [36], which can be defined by any reasonable criterion (e.g., the O-DU with the most number of O-RUs serving the user), is determined and paired with the user. We define $\mathcal{K}_u^{\text{DU}}$ to be the set of users whose PA is managed by O-DU u .

Example 1. Here we consider a scenario with $U = 3$, $M = 9$, and $K = 3$, and the sets that we have defined are illustrated in Fig. 2. Each O-DU controls three O-RUs that are closest (e.g., $\mathcal{M}_1^{\text{DU}} = \{1, 2, 3\}$), and user-centric RU clusters with $M_k^{\text{UE}} = 4$ are formed for each user (e.g., $\mathcal{M}_1^{\text{UE}} = \{1, 2, 4, 5\}$). Note that O-RU can serve multiple users (e.g., $\mathcal{K}_2^{\text{RU}} = \{1, 2\}$). Since each user needs an agent for PA, the user is paired to one of the three O-DUs (e.g., $\mathcal{K}_1^{\text{DU}} = \{1, 2\}$).

B. Time-varying Channel Model

We assume a periodic channel estimation with time interval T_e and indicate each estimation instance using index $i = 0, 1, \dots, N$. The channel between user $k \in \mathcal{K}$ and O-RU $m \in \mathcal{M}$ during channel estimation instance i is formally expressed as

$$g_{km}^{(i)} = \sqrt{\beta_{km}^{(i)}} h_{km}^{(i)}, \quad (1)$$

where $h_{km}^{(i)} = \mu_k h_{km}^{(i-1)} + \sqrt{(1 - \mu_k^2)} n_{km}^{(i)}$ is the small-scale fading factor following the first-order time-varying Gauss-Markov process for $i = 1, 2, \dots, N$. The perturbation term $n_{km}^{(i)}$ is a zero-mean, unit-variance complex Gaussian random variable independent and identically distributed (i.i.d.) over k , m , and i , i.e., $n_{km}^{(i)} \sim \mathcal{CN}(0, 1)$. At $i = 0$, we assume $h_{km}^{(0)} \sim \mathcal{CN}(0, 1)$ to be mutually independent from $n_{km}^{(1)}$. The correlation coefficient μ_k for user k is defined as $\mu_k = J_0(2\pi \frac{v_k}{c} f_c T_e)$ [38], where $J_0(\cdot)$ is the Bessel function of the first kind of order zero, v_k is the velocity of user k , f_c is the carrier frequency, and $c = 3 \times 10^8$ m/s is the speed of light. The

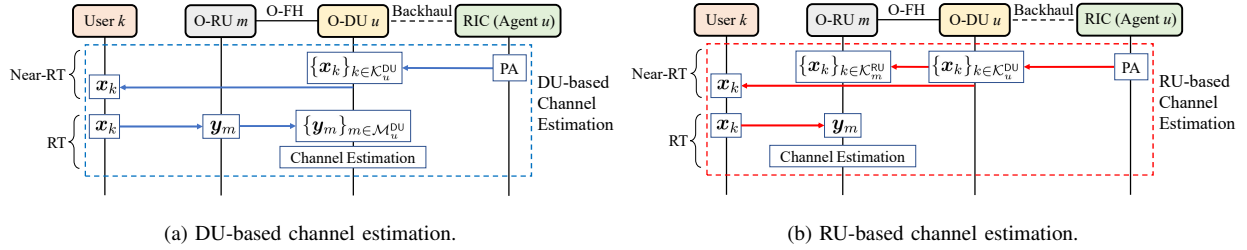


Fig. 3: A block diagram of two different channel estimation structures.

term $\beta_{km}^{(i)}$ in (1) is the large-scale fading factor inversely proportional to the distance between user k and O-RU m at the channel estimation instance i .

C. Codebook-based Channel Estimation

We consider uplink channel estimation with T_p channel uses dedicated for each estimation instance. This allows T_p orthogonal pilots to be available for channel estimation. For channel estimation, user $k \in \mathcal{K}_u^{\text{DU}}$ is assigned with one of the T_p pilots in a codebook $\mathcal{T}_u^{(i)} = \{\phi_{u,1}^{(i)}, \phi_{u,2}^{(i)}, \dots, \phi_{u,T_p}^{(i)}\}$, where each $\phi_{u,t}^{(i)}$ for $t = 1, 2, \dots, T_p$ is a unit-norm complex vector of length T_p . For each $\mathcal{T}_u^{(i)}$, we assume mutual orthogonality. Thus, for $t, t' = 1, 2, \dots, T_p$, $(\phi_{u,t}^{(i)})^H \phi_{u,t'}^{(i)} = 1$ if $t = t'$, and *zero* otherwise, where $(\cdot)^H$ denotes the conjugate transpose. We denote the pilot assigned to user k for the channel estimation instance i as $\mathbf{x}_k^{(i)}$.

To conduct channel estimation, each user $k \in \mathcal{K}$ transmits the assigned pilot $\mathbf{x}_k^{(i)}$. The signal vector (of length T_p) received by O-RU $m \in \mathcal{M}$ is then expressed as

$$\mathbf{y}_m^{(i)} = \mathbf{X}^{(i)} \mathbf{g}_m^{(i)} + \mathbf{w}_m^{(i)} = \sum_{k \in \mathcal{K}} g_{km}^{(i)} \mathbf{x}_k^{(i)} + \mathbf{w}_m^{(i)}, \quad (2)$$

where $\mathbf{X}^{(i)} = [\mathbf{x}_1^{(i)} \mathbf{x}_2^{(i)} \dots \mathbf{x}_K^{(i)}]$ is the $T_p \times K$ pilot matrix and $\mathbf{g}_m^{(i)} = [g_{1m}^{(i)} g_{2m}^{(i)} \dots g_{Km}^{(i)}]^\top$ is the channel vector (of length K) for O-RU m . Here, $\mathbf{w}_m^{(i)} \sim \mathcal{CN}(\mathbf{0}, \sigma^2 \mathbf{I}_{T_p})$ is the zero-mean complex Gaussian noise vector of length T_p with covariance $\sigma^2 \mathbf{I}_{T_p}$, where \mathbf{I}_n is the $n \times n$ identity matrix.

We discuss two different channel estimation structures within O-RAN architecture, which we illustrate in Fig. 3. One structure (Fig. 3a) performs channel estimation at O-DU whereas the estimation occurs at O-RU in the other structure (Fig. 3b). For the DU-based channel estimation, $\mathbf{y}_m^{(i)}$ from each O-RU $m \in \mathcal{M}_u^{\text{DU}}$ must be collected by the O-DU in RT scale, significantly increasing the scheduling and data transfer overhead on O-FH as the number of O-RUs grows. Such an increasing overhead is critical for the scalability of CFmMIMO. On the other hand, channel estimation at O-RU only requires the pilot information of the served users

(i.e., $\{\mathbf{x}_k^{(i)}\}_{k \in \mathcal{K}_m^{\text{RU}}}$) to be informed to each individual O-RU in near-RT scale, which does not involve as much O-FH overhead as the DU-based estimation. Hence, similar to the work in [26], we assume our channel estimation to take place at O-RUs.

Next, in case of user-centric RU clustering, each RU $m \in \mathcal{M}$ only needs to estimate $|\mathcal{K}_m^{\text{RU}}|$ different channels (i.e., $\{g_{km}^{(i)}\}_{k \in \mathcal{K}_m^{\text{RU}}}$) associated with users in $\mathcal{K}_m^{\text{RU}}$. For estimating the channel, we consider two different techniques called *pilot-matching* [19] and *least-square* [39] estimations. If we set $\hat{\mathbf{g}}_m^{(i)} = [\hat{g}_{km}^{(i)}]_{k \in \mathcal{K}_m^{\text{RU}}}^\top$ as the $|\mathcal{K}_m^{\text{RU}}|$ -length estimated channel vector from O-RU m during the channel estimation instance i , pilot-matching and least-square estimations are expressed as

$$\hat{\mathbf{g}}_m^{(i)} = (\bar{\mathbf{X}}_m^{(i)})^H \mathbf{y}_m^{(i)} \quad (3)$$

$$\text{and } \hat{\mathbf{g}}_m^{(i)} = (\bar{\mathbf{X}}_m^{(i)})^H (\mathbf{X}^{(i)} (\mathbf{X}^{(i)})^H)^{-1} \mathbf{y}_m^{(i)}, \quad (4)$$

respectively, where $\bar{\mathbf{X}}_m^{(i)} = [\mathbf{x}_k^{(i)}]_{k \in \mathcal{K}_m^{\text{RU}}}$ is the $T_p \times |\mathcal{K}_m^{\text{RU}}|$ pilot matrix of the users served by O-RU m . Now, when some of $|\mathcal{K}_m^{\text{RU}}|$ users share the pilot, $\bar{\mathbf{X}}_m^{(i)}$ is not unitary (i.e., $(\bar{\mathbf{X}}_m^{(i)})^H \bar{\mathbf{X}}_m^{(i)} \neq \mathbf{I}_{|\mathcal{K}_m^{\text{RU}}|}$), so the least-square estimation in (4), which utilizes the pseudo-inverse term $(\mathbf{X}^{(i)} (\mathbf{X}^{(i)})^H)^{-1}$ to negate the PC, yields better estimation performance. However, in the least-square approach, since $\mathbf{X}^{(i)}$ needs to be known to every O-RU and the size of $\mathbf{X}^{(i)}$ increases linearly with K , the resulting overhead causes significant delay as the number of users grows. This motivates the pilot-matching channel estimation scheme in (3) for scalability [19]. The estimated channel $\hat{g}_{km}^{(i)}$ between O-RU m and user $k \in \mathcal{K}_m^{\text{RU}}$ is then expressed as

$$\hat{g}_{km}^{(i)} = (\mathbf{x}_k^{(i)})^H \mathbf{y}_m^{(i)} = \sum_{k' \in \mathcal{K}} g_{k'm}^{(i)} (\mathbf{x}_k^{(i)})^H \mathbf{x}_{k'}^{(i)} + (\mathbf{x}_k^{(i)})^H \mathbf{w}_m^{(i)} = g_{km}^{(i)} + \sum_{\substack{k' \in \mathcal{K} \\ k' \neq k}} g_{k'm}^{(i)} (\mathbf{x}_k^{(i)})^H \mathbf{x}_{k'}^{(i)} + (\mathbf{x}_k^{(i)})^H \mathbf{w}_m^{(i)}. \quad (5)$$

Note that the summation term in the last equality captures the effect of PC.

D. Problem Formulation

We use MSE of the channel estimation described in Sec. II-C for our PA performance metric. For user k served by the O-RUs in $\mathcal{M}_k^{\text{UE}}$, we define the MSE of the channel estimate in (5) as

$$\begin{aligned} \text{MSE}_k^{(i)} &= \mathbb{E} \left[\sum_{m \in \mathcal{M}_k^{\text{UE}}} \left| \hat{g}_{km}^{(i)} - g_{km}^{(i)} \right|^2 \right] = \sum_{m \in \mathcal{M}_k^{\text{UE}}} \mathbb{E} \left[\left| \hat{g}_{km}^{(i)} - g_{km}^{(i)} \right|^2 \right] \\ &= \sum_{m \in \mathcal{M}_k^{\text{UE}}} \mathbb{E} \left[\left| \sum_{\substack{k' \in \mathcal{K} \\ k' \neq k}} g_{k'm}^{(i)} (\mathbf{x}_k^{(i)})^H \mathbf{x}_{k'}^{(i)} + (\mathbf{x}_k^{(i)})^H \mathbf{w}_m^{(i)} \right|^2 \right] = \sum_{m \in \mathcal{M}_k^{\text{UE}}} \sum_{\substack{k' \in \mathcal{K} \\ k' \neq k}} \beta_{k'm}^{(i)} \left| (\mathbf{x}_k^{(i)})^H \mathbf{x}_{k'}^{(i)} \right|^2 + \sigma^2, \quad (6) \end{aligned}$$

where the expectation is taken over the channel and noise. The third equality holds as we substitute $\widehat{g}_{km}^{(i)}$ with (5). Next, the last equality holds since $g_{km}^{(i)}$ and $\mathbf{w}_m^{(i)}$ are i.i.d. across k and m with $\mathbb{E}[|g_{km}^{(i)}|^2] = \beta_{km}^{(i)}$ and $\mathbb{E}[\|\mathbf{w}_m^{(i)}\|_2^2] = \sigma^2$, respectively. From (6), we see that the MSE is directly proportional to the interference caused by PC, and thus can be used as an effective metric to quantify the PA performance.

Since our system involves U agents, each of which handles the PA of user $k \in \mathcal{K}_u^{\text{DU}}$, we can formulate the PA optimization problem for agent u as

$$(\mathcal{P}_u) : \min_{\{\mathbf{x}_k^{(i)}\}_{k \in \mathcal{K}_u^{\text{DU}}}} \sum_{k \in \mathcal{K}} \text{MSE}_k^{(i)} \quad (7)$$

$$\text{s.t. } \mathbf{x}_k^{(i)} \in \mathcal{T}_u^{(i)}, \quad \forall k \in \mathcal{K}_u^{\text{DU}}, \quad (8)$$

$$\|\phi_{u,t}^{(i)}\|_2^2 = 1, \quad \left(\phi_{u,t}^{(i)}\right)^H \phi_{u,t'}^{(i)} = 0 \text{ if } t \neq t', \quad \forall t, t' = 1, 2, \dots, T_p. \quad (9)$$

If $\beta_{km}^{(i)}, \forall k, m$ is known, one can directly evaluate $\sum_{k \in \mathcal{K}} \text{MSE}_k^{(i)}$ using (6) and solve \mathcal{P}_u using PA algorithms (e.g., the previous works [26]–[32]). However, in large-scale systems, such prior knowledge is often not available, and one can no longer evaluate the objective function in a straightforward manner. Suppose the knowledge is somehow available for the MSE to be evaluated, but some of these algorithms (e.g., PAs with Tabu-search [30] and Hungarian algorithm [32] having the complexities of $\mathcal{O}(N_{\text{tabu}}K^2M)$ and $\mathcal{O}(KT_p^3)$, respectively) still cannot be considered as the complexity becomes prohibitive for a large number of users. To address both issues, we propose to solve \mathcal{P}_u via a distributed learning framework, details of which are given in Sec. III. The decentralization imposed in this work allows our PA scheme to be much more scalable.

III. SCALABLE LEARNING-BASED PILOT ASSIGNMENT SCHEME FOR O-RAN CFMMIMO

In this section, we first describe how our proposed PA scheme is framed in O-RAN (Sec. III-A). Next, after providing preliminaries on MA-DRL (Sec. III-B), we design a Markov game model perceiving our PA problem (Sec. III-C), and show that the action selection in our learning framework corresponds to minimizing the PC (Theorem 1). Finally, we provide implementation details for our DRL-based PA scheme (Sec. III-D) and iterative CS algorithm (Sec. III-E).

A. Pilot Assignment Framework in O-RAN Architecture

Our learning-based PA scheme for CFmMIMO is designed based on O-RAN architecture defined in Sec. II-A. Its conceptual block diagram is illustrated in Fig. 4. Here the PA is conducted under three different O-RAN control loops which have been described earlier in Fig. 1a.

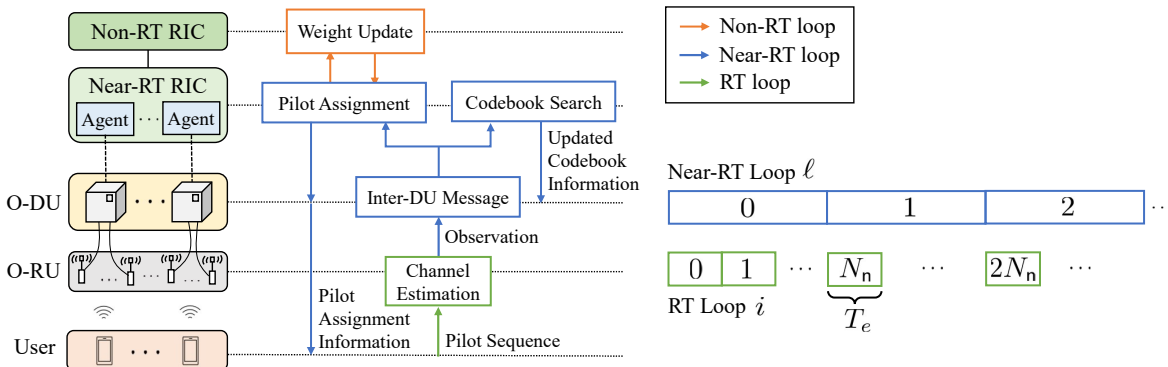


Fig. 4: A block diagram of the proposed PA scheme.

1) *RT loop*: We assume that a single round of channel estimation steps described in Sec. II-C takes place in each RT loop. Hence, we denote the index of each RT loop using the same notation used for indexing the channel estimation instance. In each RT loop i , users transmit their assigned pilots, and the O-RU m completes the channel estimation to obtain $\hat{g}_{km}^{(i)}$ for $k \in \mathcal{K}_m^{\text{RU}}$.

2) *Near-RT loop*: Near-RT loop occurs once in every N_n RT loops. During each near-RT loop, O-DU u collects observation data, which we describe later in Sec. III-C, from the O-RUs in $\mathcal{M}_u^{\text{DU}}$ and transfers it to the near-RT RIC to be used for learning. At the same time, each agent u in the near-RT RIC conducts PA on the users in $\mathcal{K}_u^{\text{DU}}$. We use $\ell = 0, 1, \dots, \lfloor \frac{N}{N_n} \rfloor$ to denote the index of near-RT loop, thus, ℓ -th near-RT loop occurs during the $N_n\ell$ -th RT loop (or the $N_n\ell$ -th channel estimation instance). The relationship between i and ℓ is visualized in Fig. 4.

To further improve our PA performance, two acceleration techniques are introduced:

- *Inter-DU message passing*: We consider inter-DU message passing which occurs at each near-RT loop. The inter-DU connection is essential for fully realizing user-centric RU clusters in decentralized CFmMIMO [36], and we exploit this feature to improve our PA performance. With inter-DU messages, we aim to reinforce the data observed by the local group of O-RUs (i.e., O-RUs of $\mathcal{M}_u^{\text{DU}}$). The details on inter-DU message passing are provided in Sec. III-D.
- *Codebook searching*: We leverage the decentralization of our system and develop a CS algorithm that operates jointly with our PA scheme. In doing so, we adopt the idea of quasi-orthogonal codebooks [40], [41] to be used across the agents. In multi-cell systems, where each cell conducts its own PA to the serving users, using non-identical orthogonal codebooks across the cells has shown improved system performance. Inspired by this, we rotate the codebook of each agent in an iterative manner to find the codebook orientation that yields the minimum

MSE of channel estimation. The detailed steps of our CS scheme is provided in Sec. III-E.

3) *Non-RT loop*: The non-RT loop is utilized to handle time-insensitive tasks. In our PA scheme, the update of the learning parameters for near-RT RIC occurs over this loop. Here, the non-RT loop occurs once in every N_{non} RT loops, and we denote $q = 0, 1, \dots, \lfloor \frac{N}{N_{\text{non}}} \rfloor$ as the non-RT loop index. As described in Fig. 1a, a near-RT loop duration can be as short as 10 ms while the shortest duration for non-RT loop is a second. Hence, we assume $N_{\text{non}} \gg N_n$.

B. Preliminaries on Multi-agent Deep Reinforcement Learning

MA-DRL addresses scenarios where multiple agents perform simultaneous decision-making based on a Markov game model [42]. For our decentralized PA problem, we define MA-DRL using a tuple $(\{\mathcal{S}_u^{(\ell)}\}_{u \in \mathcal{U}}, \{\mathbf{a}_u^{(\ell)}\}_{u \in \mathcal{U}}, \{r_u^{(\ell)}\}_{u \in \mathcal{U}})$, where $\mathcal{S}_u^{(\ell)}$, $\mathbf{a}_u^{(\ell)}$, and $r_u^{(\ell)}$ are respectively the *state*, *action*, and *reward* of the agent u during the ℓ -th near-RT loop. For each loop ℓ , agent u with a state $\mathcal{S}_u^{(\ell)}$ makes an action $\mathbf{a}_u^{(\ell)}$ to interact with the environment. Subsequently, the agent makes an observation and computes a reward $r_u^{(\ell)}$ which helps to find the next state $\mathcal{S}_u^{(\ell+1)}$.

In the non-RT loop, once an agent has completed multiple interactions with the environment, its policy on action selection for a given state is optimized by updating the weights of its respective deep neural network (DNN). Here the action is determined based on the Q-value [43] denoted by $Q(\mathcal{S}_u^{(\ell)}, \mathbf{a}_u^{(\ell)})$. The Q-value quantifies the quality of an agent's action for a given state. Thus, it is important for the agent to obtain accurate Q-values to make correct decisions. In DRL, these Q-values are computed via a DNN, the weights of which are trained with experiences so that a correct (i.e., Q-value-maximizing) action can be selected upon each decision-making.

Now, in perceiving our PA task as a multi-agent learning problem, there are two conditions we need to consider [44]. First, multiple agents making independent decisions simultaneously implies the environment is never seen as stationary to an action of a single agent. Second, due to the decentralized architecture, each agent only obtains a part of the observation available from the entire environment. Due to these conditions, in multi-agent learning, careful design of the Markov game model is crucial for achieving performance comparable to centralized learning.

C. Markov Game Model for Decentralized Pilot Assignment

In our O-RAN CFmMIMO setting, channel estimation is repeated for every RT loop i , forming a periodic interaction with the environment. The near-RT PA corresponds to action selection that affects the environment and resulting observation. Based on this, we formally define each component of the tuple presented in Sec. III-B to perceive our PA task as a Markov game model.

1) *States*: To represent the PA status of agent u on users in $\mathcal{K}_u^{\text{DU}}$ at the start of near-RT loop ℓ , we define the state as $\mathbf{S}_u^{(\ell)} = \Phi_u^{(\ell)}$ which is a $|\mathcal{K}_u^{\text{DU}}| \times T_p$ sized matrix where

$$[\Phi_u^{(\ell)}]_{k,t} = \begin{cases} 1 & \text{if } \mathbf{x}_k^{(N_n \ell)} = \phi_{u,t}^{(N_n \ell)}, \\ 0 & \text{otherwise.} \end{cases} \quad (10)$$

As discussed previously, PC occurs when users share a pilot, and this can be indicated by the *ones* in each column of $\Phi_u^{(\ell)}$. Hence, $\Phi_u^{(\ell)}$ can become an effective means to represent the condition of PA for each agent, and we aim to have the agents accurately perceive the relationship between their PA (i.e., their actions) and the resulting PC.

2) *Actions*: We consider sequential updates on the pilots, where the pilot of only a single user is changed with every action. If we consider actions that assign pilots to all $|\mathcal{K}_u^{\text{DU}}|$ users at once, this would lead our action space to take $T_p^{|\mathcal{K}_u^{\text{DU}}|}$ possible combinations and suffer from the ‘‘curse of dimensionality’’. We hence define actions as 2-tuples indicating the user of interest and the pilot to be assigned, respectively. The action of agent u at near-RT PA ℓ is formally defined as $\mathbf{a}_u^{(\ell)} = (k, t)$, where $k \in \mathcal{K}_u^{\text{DU}}$ and $t \in \{1, 2, \dots, T_p\}$. With this setting, there are total $|\mathcal{K}_u^{\text{DU}}|T_p$ possible actions for agent u to take, resulting in a more computationally scalable action space.

3) *Rewards*: We propose to compute the reward of each agent u on the ℓ -th near-RT PA based on the average sum-power of the channel estimates obtained by the O-RUs. Note that, for each action (i.e., near-RT PA) taken by an agent, N_n channel estimations are conducted by O-RU m to acquire a set of $\hat{\mathbf{g}}_m^{(i)}$ for $N_n \ell \leq i < N_n(\ell + 1)$. Using this information, O-RU m computes

$$p_{km}^{(\ell)} = \frac{1}{N_n} \sum_{n=0}^{N_n-1} \left| \hat{\mathbf{g}}_{km}^{(N_n \ell + n)} \right|^2 \quad (11)$$

on user $k \in \mathcal{K}_m^{\text{RU}}$ during the near-RT loop ℓ and sends it to the corresponding O-DU. At the end of this transfer, O-DU u collects different sets of $p_{km}^{(\ell)}$ from each O-RU $m \in \mathcal{M}_u^{\text{DU}}$ (i.e., $\{\{p_{km}^{(\ell)}\}_{k \in \mathcal{K}_m^{\text{RU}}}\}_{m \in \mathcal{M}_u^{\text{DU}}}$). In decentralized PA, each agent $u \in \mathcal{U}$ is responsible for a disjoint subset of K users, and it is desirable for the agent to have access to $p_{km}^{(\ell)}$ from all O-RUs associated with the users (i.e., $\{\{p_{km}^{(\ell)}\}_{m \in \mathcal{M}_k^{\text{UE}}}\}_{k \in \mathcal{K}_u^{\text{DU}}}$). However, as each O-DU u is only connected to O-RUs of $\mathcal{M}_u^{\text{DU}}$, $\{\{p_{km}^{(\ell)}\}_{m \in \mathcal{M}_k^{\text{UE}} \cap \mathcal{M}_u^{\text{DU}}}\}_{k \in \mathcal{K}_u^{\text{DU}}}$ only gets collected by the agent. Hence, O-DU u ends up computing the observation data to be transferred to the agent u as $\bar{p}_u^{(\ell)} = \sum_{k \in \mathcal{K}_u^{\text{DU}}} \sum_{m \in \mathcal{M}_k^{\text{UE}} \cap \mathcal{M}_u^{\text{DU}}} p_{km}^{(\ell)}$.

Note that the rest of information required by agent u (i.e., $\{\{p_{km}^{(\ell)}\}_{m \in \mathcal{M}_k^{\text{UE}} \setminus \mathcal{M}_u^{\text{DU}}}\}_{k \in \mathcal{K}_u^{\text{DU}}}$) has been collected by other O-DUs. As mentioned earlier in Sec. III-A, since we consider inter-DU

messages, this information can be transferred to each corresponding O-DU. Then, each O-DU u can now compute the reinforced observation data which is expressed as

$$\tilde{p}_u^{(\ell)} = \bar{p}_u^{(\ell)} + \sum_{k \in \mathcal{K}_u^{\text{DU}}} \sum_{m \in \mathcal{M}_k^{\text{UE}} \setminus \mathcal{M}_u^{\text{DU}}} p_{km}^{(\ell)} = \sum_{k \in \mathcal{K}_u^{\text{DU}}} \sum_{m \in \mathcal{M}_k^{\text{UE}}} p_{km}^{(\ell)}. \quad (12)$$

The observation data computed by O-DU u in (12) is transferred to agent u via backhaul, and the reward for agent u at near-RT loop ℓ is subsequently computed using the mapping function

$$r_u^{(\ell)}(p) = (p_{\max} - p)/(p_{\max} - p_{\min}), \quad (13)$$

where $p = \tilde{p}_u^{(\ell)}$ by the availability of inter-DU message. The mapping function (13) converts the observation data into a reward range such that lower values of p are rewarded higher. Here $[p_{\min}, p_{\max}]$ is the range of observation data, which we assume is set by the non-RT RIC.

We now show that the learning via our Markov model leads to taking an action that minimizes the degree of PC. The basic mechanism of learning we utilize is that, for each given state \mathcal{S}_u , we want the agent u to select the action that maximizes its Q-value [43], i.e.,

$$\mathbf{a}_u^* = \arg \max_{\mathbf{a}_u \in \mathcal{A}_u} Q(\mathcal{S}_u, \mathbf{a}_u), \quad (14)$$

where \mathcal{A}_u is the set of all possible actions for agent u . The training in DRL is done by updating the network weights via regression toward the experiences obtained. The Q-value, which is the numerical output of the trained network, is then expected to follow the average of these experiences, i.e., the Q-value is updated through training to yield $Q(\mathcal{S}_u, \mathbf{a}_u) = \mathbb{E}[r_u(p)|(\mathcal{S}_u, \mathbf{a}_u)]$.

For each near-RT loop ℓ , the following theorem shows that, with inter-DU message passing, the action selected via (14) is the best action in terms of minimizing the degree of local PC.

Theorem 1. With $\tilde{p}_u^{(\ell)}$ available, for a given state $\mathcal{S}_u^{(\ell)}$, taking the action $\mathbf{a}_u^{(\ell)}$ which satisfies (14) is equivalent to finding the action that minimizes the degree of pilot contamination occurring on local users in $\mathcal{K}_u^{\text{DU}}$ during the near-RT loop ℓ , which is expressed as

$$\sum_{k \in \mathcal{K}_u^{\text{DU}}} \sum_{m \in \mathcal{M}_k^{\text{UE}}} \sum_{n=0}^{N_n-1} \sum_{k' \in \mathcal{K}, k' \neq k} \beta_{k'm}^{(N_n \ell + n)} \left| (\mathbf{x}_k^{(N_n \ell)})_{\text{H}} \mathbf{x}_{k'}^{(N_n \ell)} \right|^2. \quad (15)$$

Proof. First, in terms of the parameters defined in our model, we find the expected reward at near-RT loop ℓ for a given state-action pair $(\mathcal{S}_u^{(\ell)}, \mathbf{a}_u^{(\ell)})$, which is expressed as

$$\mathbb{E}[r_u^{(\ell)}(\tilde{p}_u^{(\ell)})|(\mathcal{S}_u^{(\ell)}, \mathbf{a}_u^{(\ell)})] = \frac{p_{\max} - \mathbb{E}[\tilde{p}_u^{(\ell)}]}{p_{\max} - p_{\min}}, \quad (16)$$

where the equality holds from (13). Recalling (14), the learning conducted at each agent u aims to find the action achieving the maximum Q-value $Q(\mathcal{S}_u, \mathbf{a}_u)$, which we discussed to yield $\mathbb{E}[r_u(p)|(\mathcal{S}_u, \mathbf{a}_u)]$. Thus, the action selection mechanism of agent u can be expressed as

$$\mathbf{a}_u^{(\ell)} = \arg \max_{\mathbf{a}_u \in \mathcal{A}_u} \mathbb{E}[r_u^{(\ell)}(\tilde{p}_u^{(\ell)})|(\mathcal{S}_u^{(\ell)}, \mathbf{a}_u)]. \quad (17)$$

Now combining (16) and (17), we can say that

$$\mathbf{a}_u^{(\ell)} = \arg \min_{\mathbf{a}_u \in \mathcal{A}_u} \sum_{k \in \mathcal{K}_u^{\text{DU}}} \sum_{m \in \mathcal{M}_k^{\text{UE}}} \mathbb{E}[p_{km}^{(\ell)}] = \arg \min_{\mathbf{a}_u \in \mathcal{A}_u} \frac{1}{N_n} \sum_{k \in \mathcal{K}_u^{\text{DU}}} \sum_{m \in \mathcal{M}_k^{\text{UE}}} \sum_{n=0}^{N_n-1} \mathbb{E} \left[\left| \hat{g}_{km}^{(N_n \ell + n)} \right|^2 \right], \quad (18)$$

where the first and second equalities are obtained using (12) and (11), respectively. Now, for $n = 0, 1, \dots, N_n - 1$, using (5) we have

$$\begin{aligned} \mathbb{E} \left[\left| \hat{g}_{km}^{(N_n \ell + n)} \right|^2 \right] &= \mathbb{E} \left[\left| g_{km}^{(N_n \ell + n)} \right|^2 \right] + \sum_{\substack{k' \in \mathcal{K} \\ k' \neq k}} \mathbb{E} \left[\left| g_{k'm}^{(N_n \ell + n)} (\mathbf{x}_k^{(N_n \ell + n)})_{\text{H}} \mathbf{x}_{k'}^{(N_n \ell + n)} \right|^2 \right] \\ &\quad + \mathbb{E} \left[\left| (\mathbf{x}_k^{(N_n \ell + n)})_{\text{H}} \mathbf{w}_m^{(N_n \ell + n)} \right|^2 \right] = \beta_{km}^{(N_n \ell + n)} + \xi_{km}^{(\ell, n)} + \sigma^2, \end{aligned} \quad (19)$$

where $\xi_{km}^{(\ell, n)} = \sum_{\substack{k' \in \mathcal{K} \\ k' \neq k}} \beta_{k'm}^{(N_n \ell + n)} \left| (\mathbf{x}_k^{(N_n \ell + n)})_{\text{H}} \mathbf{x}_{k'}^{(N_n \ell + n)} \right|^2$ reflects the PC discussed in Sec. II-D. By the definition of $\hat{g}_{km}^{(i)}$ in (5), taking the expectation of $|\hat{g}_{km}^{(i)}|^2$ leaves only the autocorrelation terms for $\hat{g}_{km}^{(i)}$ and $\mathbf{w}_m^{(i)}$, corresponding to $\beta_{km}^{(N_n \ell + n)} = \mathbb{E}[|g_{km}^{(N_n \ell + n)}|^2]$ and $\sigma^2 = \mathbb{E}[|(\mathbf{x}_k^{(N_n \ell + n)})_{\text{H}} \mathbf{w}_m^{(N_n \ell + n)}|^2]$ in (19). This is because the channel and noise are assumed uncorrelated across k and m .

Now, since (i) $\xi_{km}^{(\ell, n)}$ is the only term that is impacted by action \mathbf{a}_u , i.e., $\beta_{km}^{(N_n \ell + n)}$ and σ^2 in (19) are independent from PA and (ii) $\mathbf{x}_k^{(i)}$ only changes once every N_n RT loops, i.e., $\mathbf{x}_k^{(N_n \ell + n)}$ is fixed for $n = 0, 1, \dots, N_n - 1$, by ignoring $\frac{1}{N_n}$ as a scaling factor, (18) is equivalent to

$$\mathbf{a}_u^{(\ell)} = \arg \min_{\mathbf{a}_u \in \mathcal{A}_u} \sum_{k \in \mathcal{K}_u^{\text{DU}}} \sum_{m \in \mathcal{M}_k^{\text{UE}}} \sum_{n=0}^{N_n-1} \sum_{k' \in \mathcal{K}, k' \neq k} \beta_{k'm}^{(N_n \ell + n)} \left| (\mathbf{x}_k^{(N_n \ell)})_{\text{H}} \mathbf{x}_{k'}^{(N_n \ell)} \right|^2, \quad (20)$$

which represents the degree of PC at near-RT loop ℓ over the users in $\mathcal{K}_u^{\text{DU}}$. ■

From Theorem 1, we conclude that learning based on our Markov games model is equivalent to performing the pilot update which minimizes the interference due to PC at each near-RT PA. According to (15), the PA made at each near-RT loop ℓ couples with the pathloss occurring over the corresponding N_n RT loops. Since we do not assume prior knowledge on the pathloss $\beta_{km}^{(i)}$, we cannot evaluate the exact MSE. However, through the reward we define and the learning mechanism of DRL, we can still design our PA scheme such that the MSE performance is

Algorithm 1: Proposed Pilot Assignment (PA) Scheme

- 1 **Input:** Pilot length T_p , number of RT loops N , number of RT loops per near-RT loop N_n , number of internal loops L , set of users managed by O-DU u $\mathcal{K}_u^{\text{DU}}$, set of O-RUs managed by O-DU u $\mathcal{M}_u^{\text{DU}}$, set of users served by O-RU m $\mathcal{K}_m^{\text{RU}}$, set of O-RUs serving the user k $\mathcal{M}_k^{\text{UE}}$, training period, update period
 - 2 Initialize near-RT loop index $\ell = 0$; randomize the parameter vectors $\boldsymbol{\theta}_u^{\text{tr}}$ and $\boldsymbol{\theta}_u^{\text{ta}}$
 - 3 Generate codebook $\mathcal{T}_u^{(N_n \ell)}$; randomly assign $\{\phi_k^{(N_n \ell)}\}_{k \in \mathcal{K}_u^{\text{DU}}}$
 - 4 **for** $\ell = 0$ **to** N **do**
 - 5 Compute $\mathbf{S}_u^{(\ell)}$ using (10)
 - 6 **if** $\ell > 0$ **then**
 - 7 Compute $r_u^{(\ell-1)}(\tilde{p}_u^{(\ell-1)})$ using (13); store $(\mathbf{S}_u^{(\ell-1)}, \mathbf{a}_u^{(\ell-1)}, r_u^{(\ell-1)}(\tilde{p}_u^{(\ell-1)}), \mathbf{S}_u^{(\ell)})$ in the memory
 - 8 **for** $l = 0$ **to** $L - 1$ **do**
 - 9 Select $\mathbf{a}_{\text{int},u}^{(\ell,l)}$ randomly; compute $\mathbf{S}_{\text{int},u}^{(\ell,l)}$ using (10); compute $r_{\text{int},u}^{(\ell,l)}$ using (22)
 - 10 Store $(\mathbf{S}_u^{(\ell)}, \mathbf{a}_{\text{int},u}^{(\ell,l)}, r_{\text{int},u}^{(\ell,l)}, \mathbf{S}_{\text{int},u}^{(\ell,l)})$ in the memory
 - 11 **if** ϵ -greedy **then** select $\mathbf{a}_u^{(\ell)}$ randomly **else** $\mathbf{a}_u^{(\ell)} = \arg \max_{\mathbf{a}_u} Q_{\boldsymbol{\theta}_u^{\text{tr}}}(\mathbf{S}_u^{(\ell)}, \mathbf{a}_u)$
 - 12 Update the PA according to $\mathbf{a}_u^{(\ell)}$
 - 13 **for** $i = 0$ **to** $N_n - 1$ **do**
 - 14 User $k \in \mathcal{K}_u^{\text{DU}}$ transmits $\phi_k^{(N_n \ell + i)}$; O-RU $m \in \mathcal{M}_u^{\text{DU}}$ estimates $\{\hat{g}_{km}^{(i)}\}_{k \in \mathcal{K}_m^{\text{RU}}}$ using (5)
 - 15 **if** $\text{mod}(\ell, \text{training period}) = 0$ **then** generate a batch from the memory and train $\boldsymbol{\theta}_u^{\text{tr}}$ via SGD on (21)
 - 16 **if** $\text{mod}(\ell, \text{update period}) = 0$ **then** set $\boldsymbol{\theta}_u^{\text{ta}} = \boldsymbol{\theta}_u^{\text{tr}}$
 - 17 **Output:** Updated pilot sequences $\{\phi_k^{(N)}\}_{k \in \mathcal{K}_u^{\text{DU}}}$
-

Non-RT DNN Training: The learning of each agent u is carried out by two DNNs called the *train* and *target* networks [33], [45], where their network parameter vectors are denoted by $\boldsymbol{\theta}_u^{\text{tr}}$ and $\boldsymbol{\theta}_u^{\text{ta}}$, respectively. Once enough experiences have been collected in the memory, a *mini-batch* of size D_b is randomly selected from the memory and used to update $\boldsymbol{\theta}_u^{\text{tr}}$ minimizing the loss:

$$L(\boldsymbol{\theta}_u^{\text{tr}}) = \mathbb{E}_\ell [y_\ell - Q_{\boldsymbol{\theta}_u^{\text{tr}}}(\mathbf{S}_u^{(\ell)}, \mathbf{a}_u^{(\ell)})], \quad (21)$$

where $y_\ell = r_u^{(\ell)} + \gamma \max_{\mathbf{a}} Q_{\boldsymbol{\theta}_u^{\text{ta}}}(\mathbf{S}_u^{(\ell+1)}, \mathbf{a})$ with γ being the discount factor. Here $Q_{\boldsymbol{\theta}}(\mathbf{S}, \mathbf{a})$ represents the Q-value for a given pair of state \mathbf{S} and action \mathbf{a} computed via a DNN of weight vector $\boldsymbol{\theta}$. The update is done using stochastic gradient descent (SGD). Here, the weights of $\boldsymbol{\theta}_u^{\text{tr}}$ are periodically copied to target network $\boldsymbol{\theta}_u^{\text{ta}}$, with the length of this period as a design parameter.

Experience generation: By the O-RAN capability, the value of N_n can vary and impact the

rate of experiences being collected to each agent, i.e., the number of experiences collected for a given amount of time varies by N_n . If N_n is too large, a sufficient size of data required to perform effective training may not be collected within a desired time period. To resolve the issue and utilize time more efficiently, we exploit the architecture of O-RAN and introduce an internal experience-generating loop inside the near-RT RIC. This internal loop is executed L times during a single near-RT loop. In particular, once an experience is obtained via the ℓ -th near-RT loop, we generate L extra experiences by taking a random action and evaluating the corresponding reward for each internal loop. We define the reward by the l -th internal loop of the ℓ -th near-RT PA as

$$r_{\text{int},u}^{(\ell,l)}(p) = (1 - \kappa_u^{(\ell,l)}/\kappa_{\text{max}}) r_u^{(\ell)}(p), \quad (22)$$

where $\kappa_u^{(\ell,l)} = \left| \sum_{t=1}^{T_p} \left(\sum_{k \in \mathcal{K}_u^{\text{DU}}} (\phi_{u,t}^{(N_n \ell)})^H \mathbf{x}_k^{(\ell,l)} - \left\lfloor \frac{|\mathcal{K}_u^{\text{DU}}|}{T_p} \right\rfloor \right) \right|$ is the penalty for having more than necessary number of users sharing the same pilot sequence and $\kappa_{\text{max}} = 2|\mathcal{K}_u^{\text{DU}}|(T_p - 1)/T_p$ is the maximum penalty obtainable. Integrating this internal loop alongside near-RT PA, we can generate L more experiences to accelerate the convergence of our scheme and train our DNNs to favor sequence combinations that have more evenly spread number of users across T_p sequences.

E. Iterative Codebook Search (CS) Algorithm

We describe our CS algorithm that is designed to work with the PA scheme in Sec. III-D. As each agent assigns pilots to its local users using the codebook $\mathcal{T}_u^{(i)}$, CS is iteratively conducted so that the final set of U codebook sets, when combined with our PA solution, suppresses the PC to the minimum degree. We detail each of the steps in the following.

First, we assign each agent $u \in \mathcal{U}$ with an identical codebook, i.e., $\mathcal{T}_1^{(0)} = \mathcal{T}_2^{(0)} = \dots = \mathcal{T}_U^{(0)}$, and initiate our PA scheme without CS to ensure that the agents first learn and improve their PA only based on the interference resulted from pilot sharing. We design our algorithm to begin its iterative CS only after the learning on PA is stabilized so that the PA and CS do not impair each other from converging. We determine the PA of agent u to be stable when the state $\mathcal{S}_u^{(\ell)}$ remains unchanged over N_{cs} near-RT loops. Once the agent u has given the same PA for N_{cs} consecutive times at the end of near-RT loop ℓ_u^* , the agent is perceived as stable and becomes subject for CS. Note that ℓ_u^* is likely to vary for each agent due to our decentralized PA framework.

If we design our agents to conduct CS in parallel, it becomes difficult to accurately evaluate a codebook as multiple actions simultaneously affect the environment. Hence, we propose to have each agent take a turn and conduct CS while the rest of agents is paused from the search. To

implement a such design, we define an operation called the CS run in which an isolated CS is conducted for each agent $u \in \mathcal{U}_{\text{CS}}^{(v)}$, where $\mathcal{U}_{\text{CS}}^{(v)}$ is the set of agents subject for CS during the v -th CS run. For each isolated search, the following steps are performed.

Suppose it is the turn of the w -th element of $\mathcal{U}_{\text{CS}}^{(v)}$, denoted by $u_{v,w}$, to perform the isolated CS, where $w = 1, 2, \dots, |\mathcal{U}_{\text{CS}}^{(v)}|$. We first define $\ell_{v,w}$ to be the near-RT loop in which the agent $u_{v,w}$ begins its search. We also let N_s define the number of near-RT loops to be spent for codebook evaluation. During the first N_s near-RT loops (i.e., $\ell_{v,w} \leq \ell < \ell_{v,w} + N_s$), the quality of current codebook matrix $\mathbf{T}_{v,w}^{\text{old}} = [\phi_{u_{v,w},1}^{(N_n \ell_{v,w})}, \phi_{u_{v,w},2}^{(N_n \ell_{v,w})}, \dots, \phi_{u_{v,w},T_p}^{(N_n \ell_{v,w})}]$ is evaluated by computing

$$\bar{r}_{v,w}^{\text{old}} = \frac{1}{N_s} \sum_{n=0}^{N_s-1} r_{u_{v,w}}^{(\ell_{v,w}+n)}(p), \quad (23)$$

which is the average of the most N_s recent rewards collected at agent $u_{v,w}$ via our PA algorithm. Note that (23) represents the quality of PA performed using the codebook $\mathcal{T}_{u_{v,w}}^{(N_n \ell_{v,w})}$.

After obtaining (23), the agent generates a $T_p \times T_p$ column-normalized random perturbation matrix $\mathbf{P}_{v,w}$ and computes the rotation matrix as $\mathbf{R}_{v,w} = \sqrt{1 - \eta_{u_{v,w}}^2} \mathbf{I}_{T_p} + \eta_{u_{v,w}} \mathbf{P}_{v,w}$, where $\eta_{u_{v,w}} = 1 - \frac{\ell_{v,w} - \ell_{u_{v,w}}^*}{N/N_n - \ell_{u_{v,w}}^*}$ is the perturbation degree designed to decrease with $\ell_{v,w}$ so that a converged solution is obtained. Note that larger $\eta_{u_{v,w}}$ results in $\mathbf{R}_{v,w}$ with greater perturbation.

After acquiring $\mathbf{R}_{v,w}$, the agent rotates the current codebook to obtain a new codebook matrix

$$\mathbf{T}_{v,w}^{\text{new}} = \text{proj}(\mathbf{R}_{v,w} \mathbf{T}_{v,w}^{\text{old}}), \quad (24)$$

where $\text{proj}(\cdot)$ is the projection function for which we use the Gram-Schmidt orthogonalization algorithm [46]. The set of T_p columns in $\mathbf{T}_{v,w}^{\text{new}}$ is then used as a new codebook for agent $u_{v,w}$ during the next N_s near-RT loops (i.e., $\ell_{v,w} + N_s \leq \ell < \ell_{v,w} + 2N_s$). After these N_s near-RT loops, where a set of N_s rewards using the new codebook are collected by our PA algorithm, the agent computes

$$\bar{r}_{v,w}^{\text{new}} = \frac{1}{N_s} \sum_{n=N_s}^{2N_s-1} r_{u_{v,w}}^{(\ell_{v,w}+n)}(p), \quad (25)$$

to evaluate the quality of the new codebook. At this point, agent $u_{v,w}$ has evaluated (23) and (25) from using two different codebooks $\mathbf{T}_{v,w}^{\text{old}}$ and $\mathbf{T}_{v,w}^{\text{new}}$, respectively, and determines which codebook to keep by the end of search using the following criterion

$$\mathbf{T}_{u_{v,w}}^{(N_n(\ell_{v,w}+2N_s))} = \begin{cases} \mathbf{T}_{v,w}^{\text{new}} & \text{if } \bar{r}_{v,w}^{\text{new}} > \bar{r}_{v,w}^{\text{old}}, \\ \mathbf{T}_{v,w}^{\text{old}} & \text{otherwise.} \end{cases} \quad (26)$$

Algorithm 2: Proposed Codebook Search (CS) Scheme

```

1 Input: Pilot length  $T_p$ , number of consistent PAs required for stability  $N_{cs}$ , codebook evaluation interval  $N_s$ ,
   number of RT loops  $N$ , set of agents  $\mathcal{U}$ 
2 Initialize CS run index  $v = 0$ , set of agents subject for CS  $\mathcal{U}_{cs}^{(v)} = \emptyset$ , the counter for agent  $u$   $a_u = 0$ ,
    $CS_{run} = 0$ , and  $CS_{iso} = 0$ ; assign identical codebook for all  $u \in \mathcal{U}$ ; capture  $\mathcal{S}_u^{(0)}$  using (10)
3 for  $\ell = 1$  to  $N$  do
4   for  $u \in \mathcal{U}$  do
5     Capture  $\mathcal{S}_u^{(\ell)}$  using (10)
6     if  $\mathcal{S}_u^{(\ell)} = \mathcal{S}_u^{(\ell-1)}$  then  $a_u = a_u + 1$  else  $a_u = 0$ ; if  $a_u = N_{cs}$  then  $\ell_u^* = \ell$ 
7   if  $CS_{run} = 0$  then
8      $\mathcal{U}_{cs}^{(v)} = \{u \in \mathcal{U} | \ell_u^* < \ell\}$ ; if  $|\mathcal{U}_{cs}^{(v)}| > 0$  then  $w = 1$  and  $CS_{run} = 1$ 
9   if  $CS_{run} = 1$  then
10    if  $CS_{iso} = 0$  then  $\ell_{v,w} = \ell$ ;  $CS_{iso} = 1$ 
11    if  $CS_{iso} = 1$  then
12      if  $\ell = \ell_{v,w} + N_s - 1$  then compute  $\bar{r}_{v,w}^{old}$  using (23); apply new codebook  $\mathbf{T}_{v,w}^{new}$  using (24)
13      if  $\ell = \ell_{v,w} + 2N_s - 1$  then
14        Compute  $\bar{r}_{v,w}^{new}$  using (25); decide codebook using (26);  $w = w + 1$  and  $CS_{iso} = 0$ 
15      if  $w > |\mathcal{U}_{cs}^{(v)}|$  then  $v = v + 1$ ;  $CS_{run} = 0$ 
16 Output: Rotated codebook  $\mathcal{T}_u^{(N)}$ ,  $\forall u \in \mathcal{U}$ 

```

As the CS described above runs for each agent in $\mathcal{U}_{cs}^{(v)}$, total $2N_s|\mathcal{U}_{cs}^{(v)}|$ near-RT loops are spent to complete the CS run v . For every run, each agent tries a new codebook generated using a random rotation and decides to keep whichever codebook that yields higher reward. The algorithm starts its very first CS run at $\ell = \min_{u \in \mathcal{U}} \ell_u^*$ and continuously conducts each subsequent CS run. By changing the codebook only when it is determined to be better, the algorithm proceeds to find the best set of U codebooks that minimizes the degree of PC. Note that, in order to evaluate the codebooks, our CS scheme utilizes the reward $r_u^{(\ell)}(p)$, which is obtained during our PA scheme. Therefore, no additional information needs to be collected the O-DUs to conduct the CS. The overall procedure for our CS scheme is summarized in Alg 2.

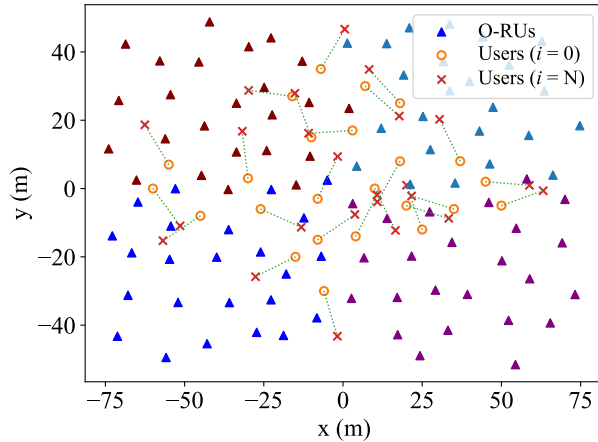


Fig. 6: Geographical layout of O-RAN CFmMIMO with $U = 4$, $M = 96$, and $K = 24$. O-RUs connected to the same O-DU have the same color. Each user moves from the initial (circle) to the final position (cross) in 10 seconds.

IV. NUMERICAL EVALUATION

In this section, we evaluate our pilot assignment (PA) scheme under O-RAN CFmMIMO channel estimation scenarios with various system parameters. We analyze both channel estimation performance and computational complexity to discuss the scalability and practicality of our method. In addition, we compare the performance of our proposed approach against different baselines which include [30], [32] among others.

A. Simulation Setup, Performance Metrics, and Baselines

We consider different combinations of O-DUs ($U = 4$), single-antenna O-RUs ($M = 96$), and single-antenna users ($K \in \{24, 36\}$) placed in an area of $100 \text{ m} \times 150 \text{ m}$ geometry to create O-RAN CFmMIMO systems. We assume the same number of O-RUs connected to each O-DU (i.e., $|\mathcal{M}_u^{\text{DU}}| = \frac{M}{U}, \forall u$) and the same number of users paired with each agent in the near-RT RIC (i.e., $|\mathcal{K}_u^{\text{DU}}| = \frac{K}{U}, \forall u$). We set channel estimation interval $T_e = 1 \text{ ms}$, implying our O-RAN RT loop occurs once every 1 ms. Each scenario is simulated with maximum $N = 10000$ RT loops, which corresponds to 10 seconds with $T_e = 1 \text{ ms}$. We assume $N_n = 10$ RT loops to occur per O-RAN near-RT loop and $L = 9$ internal experience generation per near-RT loop unless stated otherwise. For mobile scenarios, we generate initial ($i = 0$) and final ($i = N$) positions for each user such that the velocity v_k ranges from 0 m/s (or 0 km/h) to 1.4 m/s (or 5 km/h). Then, for each $i = 0, 1, \dots, N$, the position of each user is updated according to v_k . Such a mobile scenario for 96×24 CFmMIMO (where $M \times K$ refers to M O-RUs and K users) with

$U = 4$ O-DUs (equivalently, $U = 4$ agents in the near-RT RIC) is demonstrated in Fig. 6. The large-scale fading factor $\beta_{km}^{(i)}$, $\forall k, m$ is assumed to follow the 3GPP urban-micro line-of-sight pathloss model [47] with carrier frequency $f_c = 2$ GHz, O-RU height of 10 m, and user height of 1.5 m. We consider a pilot length of $T_p = 4$ and a RU cluster size of $M_k^{\text{UE}} = 8$, $\forall k$ unless stated otherwise. For our codebook search (CS) scheme, we consider an agent to be stable if the PA is consistent for $N_{\text{cs}} = 100$ consecutive times and assume the codebook evaluation interval $N_s = 5$.

We use the same DQN design for all agents: one convolutional neural network (CNN) with 32 kernels of size $|\mathcal{K}_u^{\text{DU}}| \times T_p$ followed by two fully connected layers of width $|\mathcal{K}_u^{\text{DU}}|T_p$. All layers use ReLU activation and Adam optimizer with learning rate of 0.001. The discount factor for the weight update is set $\gamma = 0.5$. We also set the size of replay memory $D_m = 1000$ and train the neural network using $D_b = 128$ samples per minibatch. The train network weights are updated via SGD and synchronized with the target network whenever 200 and 400 new additional experiences are stored in the replay memory, respectively. We implement ϵ -greedy action-selection with the probability of selecting a random action in the ℓ -th near-RT loop computed as $\epsilon_\ell = e^{-(\Gamma/N)N_n\ell}$, where $\Gamma = 15$ is the scaling factor.

We now describe the baseline methods to be simulated for performance comparison. We first consider a random assignment strategy (PA-RA) where pilots are assigned randomly for each channel estimation. The strategy does not impose any complexity but yields mediocre channel estimation performance. We also consider an exhaustive method (PA-ES) where the entire T_p^K combinations of pilots are searched to find the PA having the lowest MSE, which is evaluated using β_{km} and σ^2 assumed to be known a priori. PA-ES provides the best MSE performance but is considered impractical in terms of computational complexity as the search space exponentially increases with the number of users. We also consider two PA algorithms in the recent literature: PA strategies using Tabu-search [30] and Hungarian [32] methods. Tabu-search-based PA (PA-TS) utilizes the Tabu-search framework to find the MSE-minimizing pilot combination while the PA using the Hungarian algorithm (PA-HG) iteratively solves a reward matrix to find the PA solution. Both strategies require prior knowledge of β_{km} and σ^2 and have computational complexity that becomes prohibitive as the number of users increases. Note that these baseline methods do not consider practical framework (e.g., distributed or decentralized PA) but simply rely on a centralized processor, which makes them hard to integrate into O-RAN architecture. Also, they do not take the user mobility into account and fail to adapt to the change imposed by the

TABLE I
Comparisons of key properties among different PA algorithms

PA Algorithm	O-RAN integrated	Scalable	Decentralized	Possible without prior channel knowledge	Adaptive to mobility
PA-RA	✗	✓	✗	✓	✗
PA-TS [30]	✗	✗	✗	✗	✗
PA-HG [32]	✗	✗	✗	✗	✗
PA-ES	✗	✗	✗	✗	✗
PA-DRL + MSG	✓	✓	✓	✓	✓
PA-DRL + MSG + CBS	✓	✓	✓	✓	✓

time-varying dynamics.

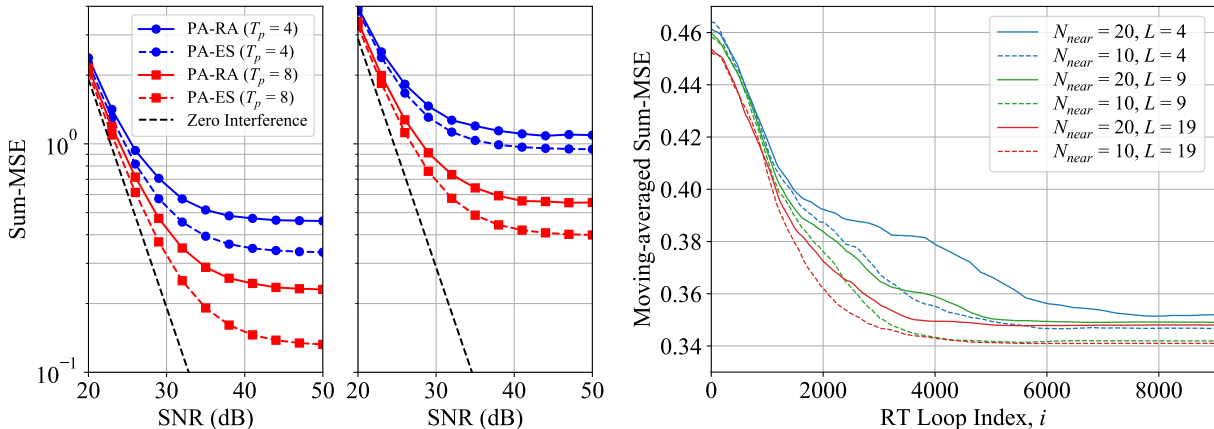
We next discuss our PA scheme to be simulated for detailed evaluation. We conduct the learning process described in Sec. III-D with inter-DU message passing (PA-DRL+MSG), i.e., $\tilde{p}_u^{(\ell)}$ is computed by each O-DU and transferred to the agent. In addition, we apply the CS scheme described in Sec. III-E along with PA-DRL+MSG (PA-DRL+MSG+CBS) to assess the improvement brought by adjusting the codebook orientation across O-DUs. As our PA scheme is specifically tailored to O-RAN architecture, practical implementation with scalable computation is possible. Since we base our learning on the DRL framework, which offers training that is adaptive to the dynamic environment, and conduct CS that checks the real-time observation, our PA scheme can reflect the user mobility. The properties of the algorithms regarding several practical aspects are summarized in Table I.

We evaluate the performance of our proposed PA scheme over two different metrics: (i) the sum-MSE defined for the objective function in \mathcal{P}_u , i.e., $\sum_{k \in \mathcal{K}} \text{MSE}_k^{(i)}$, and (ii) the runtime it takes to obtain the converged MSE. For the numerical results, we run each scenario 50 times and take their average to make our analysis statistically significant.

B. Performance of O-RAN CFmMIMO

1) *Impact of PA on channel estimation:* We first demonstrate the impact of PA on channel estimation in our O-RAN CFmMIMO system. We provide sum-MSE versus signal to noise ratio (SNR) plots for different values of T_p and K in Fig. 7a where we define SNR as $\frac{1}{\sigma^2}$.

Now we discuss several facts which are observed from the plots in Fig. 7a. First, we see that $T_p = 8$ yields lower MSE than $T_p = 4$. It is expected since the number of users sharing the same pilot tends to be smaller for larger T_p . Next, for lower SNRs, the MSE gap between PA-RA

(a) Sum-MSE vs. SNR with $K = 24$ (left) and $K = 36$ (right).(b) Sum-MSE vs. RT loop with $K = 24$.Fig. 7: Sum-MSE vs. SNR plot in terms of T_p and K (left) and sum-MSE vs. RT loop plot in terms of N_n and L (right).

and PA-ES is not significant since the noise dominantly contributes to channel estimation error. However, as SNR increases, interference due to PC becomes more dominant and forces an error floor, making the curves almost horizontal. For the case of 50 dB SNR, we find that with $T_p = 4$ and $K = 24$, optimizing PA can reduce the sum-MSE up to 27%. For the remaining experiments, we use SNR of 50 dB to focus on the interference-limited regime.

2) *Impact of O-RAN parameters:* We assess the impact of O-RAN-dependent system parameters on the performance of our PA scheme. The sum-MSE performance curves (moving-averaged with a window size of 500) of PA-DRL+MSG over the O-RAN RT loop for different values of N_n and L are shown in Fig. 7b. Recall that N_n is the number of RT loops for a single near-RT loop, and L is the number of extra experiences generated per near-RT loop by the agent. Both N_n and L are dependent on the capability of O-RAN in which CFmMIMO network is built.

Now, we make the following observations from Fig. 7b. First, regardless of the parameter values, our scheme shows stabilized (i.e., converged) sum-MSE performance, which verifies the effectiveness of our learning when implemented under O-RAN architecture. Second, a lower N_n yields improved MSE regardless of L . Here, lower N_n implies more near-RT loops during the given number of RT loops, allowing agents to interact with the environment more frequently and take more actions to find better solutions. Third, a higher L (more internal loops) allows us to achieve greater sum-MSE reduction in earlier RT loops, validating that more experiences collected in replay memory within the same period are beneficial. Thus, with greater size of datasets available, our scheme is expected to find the PA faster with low sum-MSE.

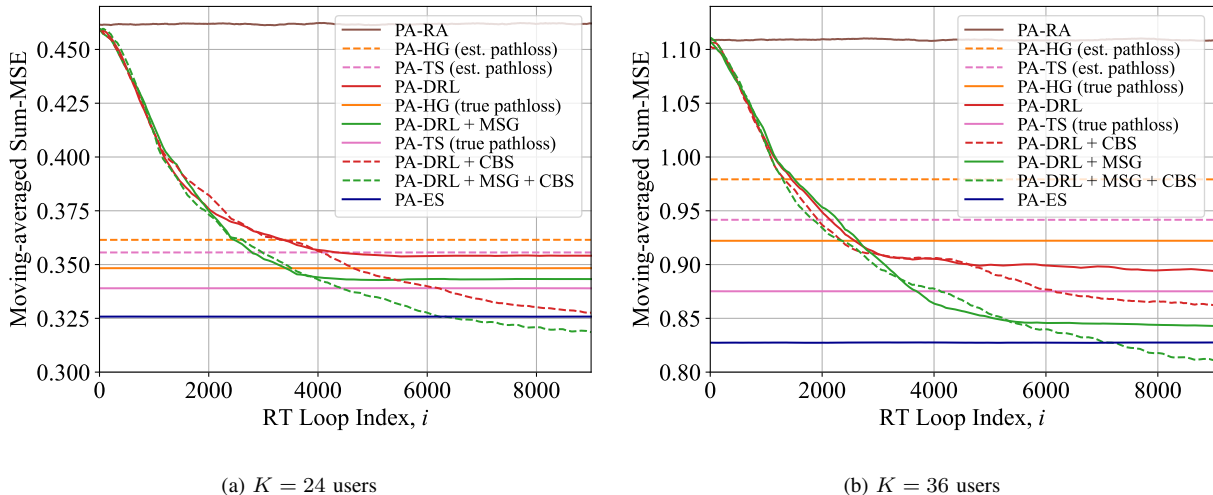


Fig. 8: Sum-MSE performance of different PA schemes over 24 stationary users (left) and 36 stationary users (right).

C. Performance Comparison Against Different Baselines

Now we assess our proposed PA scheme and compare its performance with several baselines over two metrics: channel estimation MSE and algorithm runtime.

1) *Comparison in MSE:* First, we consider static scenarios, i.e., $v_k = 0, \forall k$. The plots showing sum-MSE performance (moving-averaged with a window size of 500) over RT loops for $K = 24$ and $K = 36$ are presented in Fig. 8a and Figs. 8b, respectively. Note that the PA solutions obtained by PA-HG, PA-TS, and PA-ES required true pathloss information and were fixed for the entire RT loops. Among these approaches, it is verified from both figures that PA-ES yields much better MSE performance than PA-TS and PA-HG. We also considered the case where PA-HG and PA-TS are conducted using the estimated pathloss, which yields a considerable performance gap compared to the case of using true pathloss knowledge. Given that these baselines require prior knowledge (preferably accurate) to achieve the given performance, our learning-based PA scheme, which does not impose such requirement, is still able to show competitive performance against them. PA-DRL+MSG clearly outperforms PA-HG and PA-TS with estimated pathloss and provides comparable performance with the ones with true pathloss. Once we utilize CS scheme, our proposed PA-DRL+MSG+CBS shows significant improvement and achieves better performance than PA-ES as a result of jointly optimizing both PA and codebook orientation.

Next, we consider scenarios in which users move over time (i.e., $\beta_{km}^{(i)}$ changes over i , and $v_k > 0, \forall k \in \mathcal{K}$). Fig. 9 shows the sum-MSE performance (moving-averaged with a window size of 500) of different PA algorithms with $K = 24$ evaluated at three different user velocities:

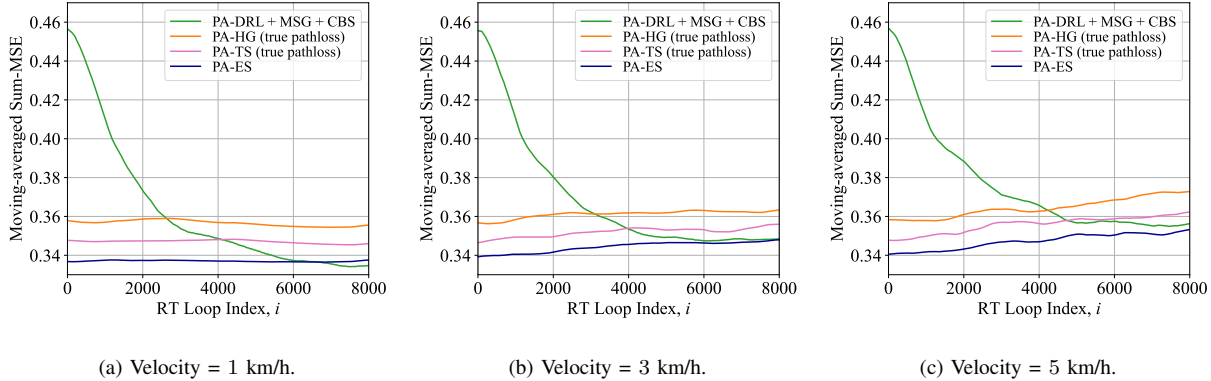


Fig. 9: MSE performance of different PA schemes over 24 mobile users with different velocities: 1 km/h, 3 km/h, and 5 km/h.

1, 3, and 5 km/h. PA solution obtained by the baselines at the beginning (i.e., $i = 0$) becomes less effective as time advances, showing a different degree of steady increase by the velocity. Unlike these baselines, as our PA and CS schemes make their decisions based on the real-time observations, in the proposed PA-DRL+MSG+CBS, PAs can be performed in an adaptive manner, maintaining its performance as shown in Fig. 9. Hence, our scheme can provide competitive performance with the prior knowledge-constrained baseline methods under a dynamic environment.

Overall, our scheme provides satisfactory performance in MSE as it exploits the decentralized architecture of O-RAN CFmMIMO via distributed learning and codebook adjustment.

2) *Comparison in algorithm runtime:* Now, we evaluate and compare the computational complexity of different PA algorithms. We first provide the runtime measurements of different PA methods with various number of users K in Fig. 10a. The complexities for PA-TS and PA-HG, which are respectively $\mathcal{O}(N_{\text{tabu}}K^2M)$ [30] and $\mathcal{O}(KT_p^3)$ [32], are confirmed by our experimental result that shows a polynomial increase. Hence, both PA-TS and PA-HG are rendered impractical when PA needs to perform over a CFmMIMO network with a growing network size. Meanwhile, our PA algorithm shows a relatively negligible increase, implying its effectiveness in scalability. The steady runtimes from our PA scheme are due to the utilization of (i) O-RAN architecture where duration-varying tasks are distributed across the network and (ii) DNNs of fixed size which only perform a forward computation to determine each pilot update step over near-RT loop. We observe a slight increase in runtime when we consider inter-DU messages into our PA scheme because generating a new set of messages imposes extra computations. Note that our CS scheme barely adds any runtime as it utilizes the rewards already computed during our PA scheme. We hence conclude that our low-complexity PA scheme is a scalable strategy that supports large-scale

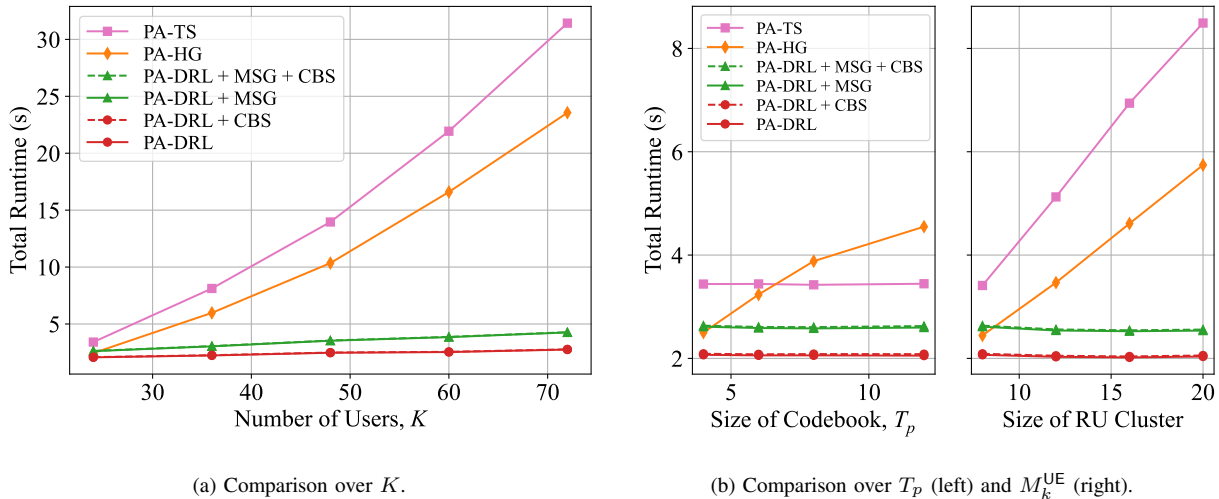


Fig. 10: Runtime comparison of different PA schemes over different K values (left) and T_p and size of RU cluster values (right).

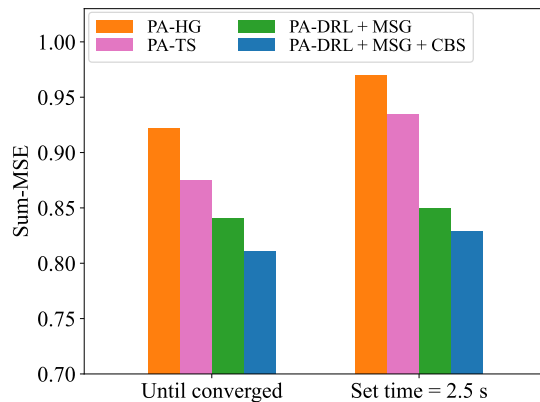


Fig. 11: Sum-MSE comparison of different PA schemes with a fixed runtime (deadline). PA-ES is not included since the considered runtime (i.e., 2.5 seconds) is too short to evaluate the reliable performance of exhaustive search.

CFmMIMO systems. Note that PA-ES, which is the best baseline in MSE minimization, requires an extreme amount of runtime as it searches over all T_p^K combinations of PA. On the other hand, PA-RA requires no extra runtime but shows much worse MSE performance than other PA schemes (Figs. 8a and 8b).

Next, we assess the total runtime required to conduct PA algorithms over different values of T_p (left) or M_k^{UE} (right) in Fig. 10b. For varying T_p (the length of pilot), only PA-HG shows undesirable behavior in complexity since the size of the reward matrix used in the Hungarian algorithm depends on T_p . With respect to M_k^{UE} (the size of RU cluster), both PA-TS and PA-HG display a linear increase. Meanwhile, our proposed scheme provides consistent runtimes for both parameters, which verifies their scalability to support a network with large system parameters.

3) *Comparison in MSE with channel estimation deadline:* We next demonstrate the impact of having a channel estimation deadline (in terms of runtime) on the MSE performance to consider practical scenarios where time resource for PA can be strictly limited. In Fig. 11, we provide a bar chart summarizing the runtime measurements for $K = 36$ stationary users in two different cases: (i) PA algorithms run until the MSE performance converges and (ii) algorithms only run for 2.5 seconds runtime. As expected, when the time constraint is imposed, every PA algorithm shows degradation in sum-MSE as compared to the case where the algorithms fully run until converged. Both PA-HG and PA-TS algorithms show significant increase in their MSE since the amount of runtime allocated is considerably lower than the runtime required for convergence. Meanwhile, our proposed PA scheme show relatively less increase in MSE due to its scalable runtime which is not impacted by the time constraint significantly. This result once again confirms the computational advantage of our PA scheme over the baseline methods.

V. CONCLUSION

In this paper, we developed a learning-based PA scheme for the decentralized CFmMIMO system framed in O-RAN. We adopted O-RAN as a practical system architecture where distinct network functions and multi-timescale control loops efficiently govern the framework of our scheme. After formulating the PA problem and designing the corresponding Markov game model, we developed a PA algorithm based on the MA-DRL framework. We also developed a CS scheme that accelerates our learning-based PA in MSE-minimization without any significant additional complexities. Compared to the state-of-the-art baselines, our approach provided satisfactory performance in terms of both channel estimation MSE and computational scalability. Furthermore, unlike most of the existing PA strategies, our scheme does not require any prior channel knowledge.

REFERENCES

- [1] M. Z. Chowdhury, M. Shahjalal, S. Ahmed, and Y. M. Jang, "6G wireless communication systems: Applications, requirements, technologies, challenges, and research directions," *IEEE Open J. the Commun. Soc.*, vol. 1, pp. 957–975, 2020.
- [2] Y. L. Lee, D. Qin, L.-C. Wang, and G. H. Sim, "6G massive radio access networks: Key applications, requirements and challenges," *IEEE Open J. Veh. Technol.*, vol. 2, pp. 54–66, 2021.
- [3] S. K. Singh, R. Singh, and B. Kumbhani, "The evolution of radio access network towards open-RAN: Challenges and opportunities," in *IEEE Wireless Commun. Netw. Conf. Workshops (WCNCW)*, 2020, pp. 1–6.
- [4] S. Niknam, A. Roy, H. S. Dhillon, S. Singh, R. Banerji, J. H. Reed, N. Saxena, and S. Yoon, "Intelligent O-RAN for beyond 5G and 6G wireless networks," 2020. [Online]. Available: <https://arxiv.org/abs/2005.08374>
- [5] M. Polese, L. Bonati, S. D'Oro, S. Basagni, and T. Melodia, "Understanding O-RAN: Architecture, interfaces, algorithms, security, and research challenges," 2022. [Online]. Available: <https://arxiv.org/abs/2202.01032>

- [6] 3GPP, “NG-RAN; architecture description,” Tech. Rep. TS 38.401 V17.2.0, Sep 2022.
- [7] O-RAN Alliance, “O-RAN architecture description,” Tech. Rep. V07.00, 2022.
- [8] M. Mohsin, J. M. Batalla, E. Pallis, G. Mastorakis, E. K. Markakis, and C. X. Mavroumoustakis, “On analyzing beamforming implementation in O-RAN 5G,” *Electronics*, vol. 10, no. 17, 2021.
- [9] T. Hewavithana, A. Chopra, B. Mondal, S. Wong, A. Davydov, and M. Majmundar, “Overcoming channel aging in massive MIMO basestations with open RAN fronthaul,” in *IEEE Wireless Commun. Netw. Conf. (WCNC)*, 2022, pp. 2577–2582.
- [10] O-RAN Alliance, “O-RAN working group 1 massive MIMO use cases,” Tech. Rep. V01.00, 2022.
- [11] 3GPP, “Study on new radio access technology: Radio access architecture and interfaces,” Tech. Rep. TR 38.801 V14.0.0, March 2017.
- [12] N.-N. Dao, Q.-V. Pham, N. H. Tu, T. T. Thanh, V. N. Q. Bao, D. S. Lakew, and S. Cho, “Survey on aerial radio access networks: Toward a comprehensive 6G access infrastructure,” *IEEE Commun. Surv. & Tut.*, vol. 23, no. 2, pp. 1193–1225, 2021.
- [13] C. Pham, F. Fami, K. K. Nguyen, and M. Cheriet, “When RAN intelligent controller in O-RAN meets multi-UAV enable wireless network,” *IEEE Trans. Cloud Comput.*, pp. 1–15, 2022.
- [14] O-RAN Alliance, “O-RAN working group 1 use cases detailed specification,” Tech. Rep. V09.00, 2022.
- [15] C. Studer, S. Medjkouh, E. Gonultas, T. Goldstein, and O. Tirkkonen, “Channel charting: Locating users within the radio environment using channel state information,” *IEEE Access*, vol. 6, pp. 47 682–47 698, 2018.
- [16] G. Interdonato, E. Björnson, H. Q. Ngo, P. Frenger, and E. G. Larsson, “Ubiquitous cell-free massive MIMO communications,” *EURASIP J. Wireless Commun. Netw.*, vol. 2019, no. 1, p. 197, 2019.
- [17] J. Zhang, S. Chen, Y. Lin, J. Zheng, B. Ai, and L. Hanzo, “Cell-free massive MIMO: A new next-generation paradigm,” *IEEE Access*, vol. 7, pp. 99 878–99 888, 2019.
- [18] J. Zhang, E. Björnson, M. Matthaiou, D. W. K. Ng, H. Yang, and D. J. Love, “Prospective multiple antenna technologies for beyond 5G,” *IEEE J. Sel. Areas Commun.*, vol. 38, no. 8, pp. 1637–1660, 2020.
- [19] E. Björnson and L. Sanguinetti, “Making cell-free massive MIMO competitive with MMSE processing and centralized implementation,” *IEEE Trans. Wireless Commun.*, vol. 19, no. 1, pp. 77–90, 2020.
- [20] H. Yang and T. L. Marzetta, “Energy efficiency of massive MIMO: Cell-free vs. cellular,” in *IEEE 87th Veh. Technol. Conf. (VTC Spring)*, 2018, pp. 1–5.
- [21] E. Björnson and L. Sanguinetti, “Scalable cell-free massive MIMO systems,” *IEEE Trans. Commun.*, vol. 68, no. 7, pp. 4247–4261, 2020.
- [22] G. Interdonato, P. Frenger, and E. G. Larsson, “Scalability aspects of cell-free massive MIMO,” in *IEEE Int. Conf. Commun. (ICC)*, 2019, pp. 1–6.
- [23] H. He, X. Yu, J. Zhang, S. H. Song, and K. B. Letaief, “Cell-free massive MIMO for 6G wireless communication networks,” *J. Commun. Inf. Netw.*, vol. 6, pp. 321–335, 2021.
- [24] H. A. Ammar, R. Adve, S. Shahbazpanahi, G. Boudreau, and K. V. Srinivas, “User-centric cell-free massive MIMO networks: A survey of opportunities, challenges and solutions,” *IEEE Commun. Surv. & Tut.*, vol. 24, no. 1, pp. 611–652, 2022.
- [25] H. Yin, D. Gesbert, and L. Cottatellucci, “Dealing with interference in distributed large-scale MIMO systems: A statistical approach,” *IEEE J. Sel. Topics Signal Process.*, vol. 8, no. 5, pp. 942–953, 2014.
- [26] H. Q. Ngo, A. Ashikhmin, H. Yang, E. G. Larsson, and T. L. Marzetta, “Cell-free massive MIMO versus small cells,” *IEEE Trans. Wireless Commun.*, vol. 16, no. 3, pp. 1834–1850, March 2017.

- [27] M. Attarifar, A. Abbasfar, and A. Lozano, "Random vs structured pilot assignment in cell-free massive MIMO wireless networks," in *IEEE Int. Conf. Commun. Workshops (ICC Workshops)*, 2018, pp. 1–6.
- [28] R. Sabbagh, C. Pan, and J. Wang, "Pilot allocation and sum-rate analysis in cell-free massive MIMO systems," in *IEEE Int. Conf. Commun. (ICC)*, 2018, pp. 1–6.
- [29] S. Chen, J. Zhang, E. Björnson, J. Zhang, and B. Ai, "Structured massive access for scalable cell-free massive MIMO systems," *IEEE J. Sel. Areas Commun.*, vol. 39, no. 4, pp. 1086–1100, 2021.
- [30] H. Liu, J. Zhang, X. Zhang, A. Kurniawan, T. Juhana, and B. Ai, "Tabu-search-based pilot assignment for cell-free massive MIMO systems," *IEEE Trans. Veh. Technol.*, vol. 69, no. 2, pp. 2286–2290, 2020.
- [31] H. Liu, J. Zhang, S. Jin, and B. Ai, "Graph coloring based pilot assignment for cell-free massive MIMO systems," *IEEE Trans. Veh. Technol.*, vol. 69, no. 8, pp. 9180–9184, 2020.
- [32] S. Buzzi, C. D'Andrea, M. Fresia, Y.-P. Zhang, and S. Feng, "Pilot assignment in cell-free massive MIMO based on the hungarian algorithm," *IEEE Wireless Commun. Lett.*, vol. 10, no. 1, pp. 34–37, 2021.
- [33] W. Li, W. Ni, H. Tian, and M. Hua, "Deep reinforcement learning for energy-efficient beamforming design in cell-free networks," in *IEEE Wireless Commun. Netw. Conf. Workshops (WCNCW)*, 2021, pp. 1–6.
- [34] F. Fredj, Y. Al-Eryani, S. Maghsudi, M. Akrouf, and E. Hossain, "Distributed beamforming techniques for cell-free wireless networks using deep reinforcement learning," *IEEE Trans. Cogn. Commun. Netw.*, vol. 8, no. 2, pp. 1186–1201, 2022.
- [35] Y. Zhao, I. G. Niemegeers, and S. M. H. De Groot, "Dynamic power allocation for cell-free massive MIMO: Deep reinforcement learning methods," *IEEE Access*, vol. 9, pp. 102 953–102 965, 2021.
- [36] V. Ranjbar, A. Girycki, M. A. Rahman, S. Pollin, M. Moonen, and E. Vinogradov, "Cell-free mMIMO support in the O-RAN architecture: A PHY layer perspective for 5G and beyond networks," *IEEE Commun. Standards Mag.*, vol. 6, no. 1, pp. 28–34, 2022.
- [37] 3GPP, "NR; radio resource control (RRC) protocol specification," Tech. Rep. TS 38.331, Sep 2022.
- [38] T. Kim, D. J. Love, and B. Clerckx, "MIMO systems with limited rate differential feedback in slowly varying channels," *IEEE Trans. Commun.*, vol. 59, no. 4, pp. 1175–1189, 2011.
- [39] Y. Liu, Z. Tan, H. Hu, L. J. Cimini, and G. Y. Li, "Channel estimation for OFDM," *IEEE Commun. Surv. & Tut.*, vol. 16, no. 4, pp. 1891–1908, 2014.
- [40] Z. Zhang, C. Wang, and H. Papadopoulos, "On-the-fly uplink training and pilot code sequence design for cellular networks," 2018. [Online]. Available: <https://arxiv.org/abs/1811.02203>
- [41] A. Chowdhury, P. Sasmal, C. R. Murthy, and R. Chopra, "On the performance of distributed antenna array systems with quasi-orthogonal pilots," *IEEE Trans. Veh. Technol.*, vol. 71, no. 3, pp. 3326–3331, 2022.
- [42] G. Qu, A. Wierman, and N. Li, "Scalable reinforcement learning for multi-agent networked systems," 2019. [Online]. Available: <https://arxiv.org/abs/1912.02906>
- [43] R. S. Sutton and A. G. Barto, *Reinforcement Learning: An Introduction*. Cambridge, MA, USA: MIT Press, 1998.
- [44] A. Feriani and E. Hossain, "Single and multi-agent deep reinforcement learning for AI-enabled wireless networks: A tutorial," *IEEE Commun. Surv. & Tut.*, 2021.
- [45] J. Ge, Y.-C. Liang, J. Joung, and S. Sun, "Deep reinforcement learning for distributed dynamic MISO downlink-beamforming coordination," *IEEE Trans. Commun.*, vol. 68, no. 10, pp. 6070–6085, 2020.
- [46] G. H. Golub and C. F. Van Loan, *Matrix Computations*, 3rd ed. The Johns Hopkins University Press, 1996.
- [47] 3GPP, "Evolved universal terrestrial radio access (E-UTRA); further advancements for E-UTRA physical layer aspects," Tech. Rep. TR 36.814 V9.2.0, March 2017.